Smart Structures and Systems, *Vol. 28, No. 4 (2021) 469-481*
https://doi.org/10.12989/sss.2021.28.4.469

Numerical investigation on cyclic behaviour of superelastic shape memory alloy (SMA) dampers

Young Chan Kim [1,2a] and Jong Wan Hu*[1,2]

[1] *Incheon Disaster Prevention Research Center, Incheon National University, Incheon 22012, South Korea*
[2] *Department of Civil and Environmental Engineering, Incheon National University, Incheon 22012, South Korea*

(*Received May 17, 2020, Revised July 2, 2021, Accepted July 9, 2021*)

Abstract. In recent decades, researchers have developed many technologies like energy dissipating dampers to improve the response of structures in seismic events but still limitations persist in earthquake-resistant design. Residual drift is still a significant problem encountered while using dampers which results in a reduction in their performance. Many types of dampers have been introduced to localize the damages in a defined section of a structure to prevent structural failure and decrease the repairing cost. However, in general, rehabilitation of a structure using a damper is not an economical option because residual deformation occurs due to limitations of constituent materials of the damper. Therefore, in this paper, a shape memory alloys (SMAs) damper is proposed to mitigate the performance degradation problem caused by residual deformation of a structure and to reduce maintenance and repairing costs. The shape memory alloys can reduce residual deformation at room temperature due to the superelastic effect. In addition, a pretension force was applied to prevent damage by reducing the fastening force of the shape memory alloy bar and to improve the load performance. Finite element analysis was performed to verify the performance of the damper to which the pretension was applied. Furthermore, recentering performance and energy dissipation capacity of the damper were analyzed. The analysis results show that the proposed damper can reduce the residual strain by recentering, as well as improve energy dissipation and ultimate capacity.

Keywords: finite element analysis (FEA); pretension force; residual deformation; shape memory alloys (SMAs); superelastic effect

1. Introduction

Modern seismic-resistant structural systems are designed by the concept that the structure must be stable and not collapse during an earthquake. Therefore, seismic-resistant structural systems should have sufficient ductility, strength, and the ability to reduce seismic energy (Massah and Dorvar 2014). Seismic resistant design is a method of resisting earthquakes due to the energy dissipation and ductility performance of the component members of the structure. However, if an earthquake exceeds the allowable performance of the structure, damage, such as cracks and plastic deformation occurs in the element member, which leads to an economic loss of replacing the member to rehabilitation the structure. In addition, the general repair and reinforcement method applied to solve the damage of the structure is uneconomical due to the additional cost problem.

Therefore, researchers are conducting research on repairing and reinforcement methods, such as smart isolation devices, cable self-centering devices, and SMA wire devices, to secure various performances of structural systems (Silwal *et al*. 2016, Mansouri *et al*. 2017, Haque and Alam 2017, Shi *et al*. 2019, Hu 2015). One of the most efficient methods for these various devices is to apply a smart material such as SMA to the damper device. The application of damper using SMA can improve seismic performance and leads to construct a structural system that can maintain economic efficiency.

Among the various seismic structural systems, the concentrically braced frames (CBFs) enhance the strength of the structure and show efficient resistance to lateral loads. The component member dissipates the energy generated due to such performance but has a disadvantage in that plastic deformation occurs due to limited lateral displacement performance due to structural characteristics. Due to the occurrence of plastic deformation, the structure cannot be reused unless the member is replaced or reinforced. Therefore, in the past decades, researchers have focused on applying smart materials such as SMA to seismic structural systems (Dezfuli and Alam 2015, Gao *et al*. 2016, Sultana and Youssef 2016, Mirzai *et al*. 2018, Zareie *et al*. 2017, Sultana and Youssef 2018, Speicher *et al*. 2017, Mirzai and Hu 2019, Zareie *et al*. 2019). To solve this problem, in this study, as shown in Fig. 1, the SMA damper is connected to the top of the inverted V-shaped bracing system and in the center of the beam member in CBFs. SMA damper reinforcement can effectively control the vibration and displacement of the seismic structural system and reduce plastic deformation. In addition, the bottom plate of the SMA damper device with a bolt hole is fixed to

*Corresponding author, Associate Professor,
E-mail: jongp24@inu.ac.kr
[a] Ph.D.

ISSN: 1738-1584 (Print), 1738-1991 (Online)

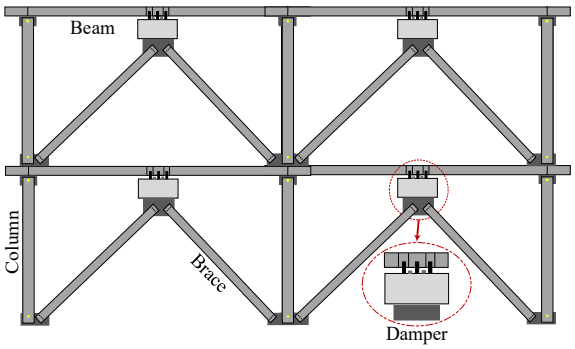

Fig. 1 Superelastic SMA dampers installed at the CBFs

the flange of the beam using bolts and nuts to exclude construction uncertainty due to welding.

In general, steel materials absorb shock from external loads such as earthquakes and have a certain level of energy dissipation by plasticity. However, there are disadvantages that require maintenance by residual deformation and damage. SMA has the strength to resist shear and bending after plastic deformation, so it has the advantage of reducing more displacement and damage when a strong external load such as an earthquake occurs in an instant. SMA has two important properties, the first is the Shape Memory Effect (SME), a unique property that recovers residual deformation due to external loads. The SME means that the material remembers the initial shape, size, and pre-deformed shape and returns to its original shape when heated. Secondly, SMA has Superelastic Effect (SE), a special ability to support high plastic deformation to recover most of the residual strain. The SE means that even if plastic deformation occurs beyond the elastic limit of the material, it can be returned to its original form only by removing the load. This particular property of the SMAs is related to the forward transformation of the SMAs from martensite to austenite during loading, and reversed transformation from austenite to martensite during unloading when the temperature is higher than austenite finish temperature (DesRoches *et al*. 2004). Fig. 2 shows the stress-strain curve showing the SME and SE of SMA. SMA exhibits a flag-shaped hysteresis under cyclic loads.

Recently, due to the development of manufacturing technology and heating methodology of SMAs, large-size SMAs have became commercially available (Qiu *et al*. 2020). In addition, SMA has recently been used in many structures due to its additional shock absorption ability by energy dissipation, excellent corrosion resistance, and resistance to fatigue destruction (Hu 2014, 2015, Hu and Choi 2014). The SMA damper is a device that improves the plastic strain reduction and energy dissipation capacity by the frictional force generated between the superelastic SMA and the member into which the pre-tension is introduced. Recentering is an important property of SMA damper, in which it gains original state after the load is removed at room temperature even if a considerable amount of plastic displacement occurs beyond the elastic limit. Recentering performance of SMA damper makes it an ideal candidate in terms of cost-effectiveness by reducing maintenance and replacement costs. The application of pretension to the SMA bar, where the stress is concentrated by the seismic load, basically reduces the bar's relaxation and prevents the separation of the joint surface of the damper part. In addition, it is possible to reduce the fatigue damage caused by the low fastening force, so that the service life can be prolonged. The application of pretension can achieve the required performance with a small number of SMA bars for the required performance of the SMA damper, and the strength and energy dissipation ability are improved compared to the general damper.

In this study, cyclic behaviour of SMA damper was investigated using Finite Element Analysis (FEA). The SMA damper was designed based on the prying action effect to reduce damage to the member caused by load concentration. The theory and technical characteristics of the damper were figured out and the concept was established. To evaluate the behaviour characteristics, 3D finite element analysis was performed according to design variables such as steel, SMA material, and pretension. For the finite element analysis results, models according to design variables were compared with each other. Finally, the analysis results were analyzed in terms of seismic performance such as ultimate strength, permanent deformation and recentering ratio.

2. Damper design

SMA damper is a smart device that has recentering as well as energy dissipation characteristics. As shown in Fig. 3, SMA damper can be divided into internal and external

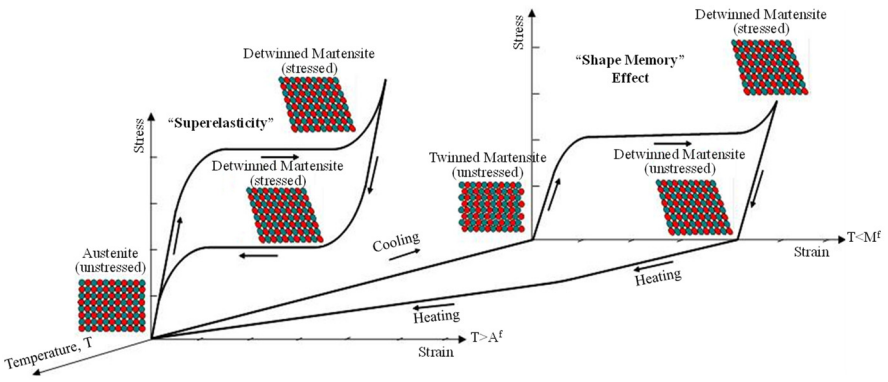

Fig. 2 Stress and strain curve for superelastic SMAs

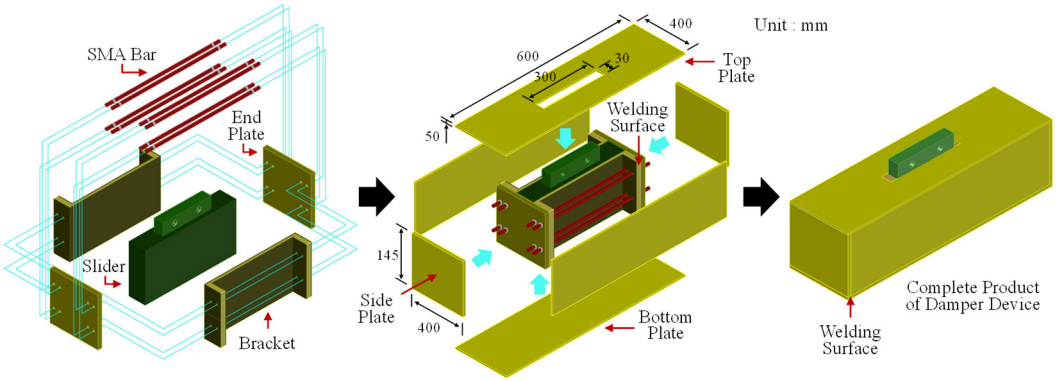

Fig. 3 3D schematic drawing for the components of SMA damper connections

parts. The internal parts of the damper consist of slider, bracket, end plate, and SMA rod. The slider is directly connected to the structure and transfers external loads to the damper. The bracket performs as a fastener for integral behaviour with boxed steel. The end plate supports the slider, bracket and SMA bar components. The SMA bars are installed by fixing it with fastening hardware, such as a nut to the end plate by passing through the bracket. SMA bars can be symmetrically adjusted according to the required strength and recentering force. According to the lateral movement of the slider due to the external load, the SMA bars behave simultaneously with the end plate. Therefore, the tension is applied in both directions about the center of the slider. In addition, even when the elasticity is exceeded, it is possible to recover to the original shape without the occurrence of residual deformation due to the recentering force of the material. The external parts are composed of four plates and the internal parts are covered and welded to complete the damper device. SMA damper is a smart device that has recentering as well as energy dissipation characteristics. As shown in Fig. 3, SMA damper can be divided into internal and external parts. The internal parts of the damper consist of slider, bracket, end plate, and SMA bar. The slider is directly connected to the structure and transfers external loads to the damper. The bracket performs as a fastener for integral behaviour with boxed steel. The end plate supports the slider, bracket and SMA bar components. The SMA bars are installed by fixing it with fastening hardware, such as a nut to the end plate by passing through the bracket. SMA bars can be symmetrically adjusted according to the required strength and recentering force. According to the lateral movement of the slider due to the external load, the SMA bars behave simultaneously with the end plate. Therefore, the tension is applied in both directions about the centre of the slider. In addition, even when the elasticity is exceeded, it is possible to recover to the original shape without the occurrence of residual deformation due to the recentering force of the material. The external parts are composed of four plates and the internal the internal parts are covered and welded to complete the damper device.

The SMA damper is formed so that the seismic load is concentrated on the SMA bars, which acts as a recentering and energy dissipation device. As shown in Fig. 4, depending on the geometry of the damper, three failure modes due to load can occur. The SMA bars to which the pretension is applied resist the bending moment (M) caused by the tension load (ΣB) and the applied load (P). All failures should be confined to the SMA bars and the other parts of the damper must maintain elastic range. Therefore, mode 3 is an ideal failure mode according to the behavior of the SMA damper. The failure mode 1 in Fig. 4(a) shows that the hinge can be formed by the plastic limit on the end plate by bending when the SMA bar is not under tension. In this failure mode damper does not work properly. On the other hand, in failure mode 2 of Fig. 4(b), bending of end plate

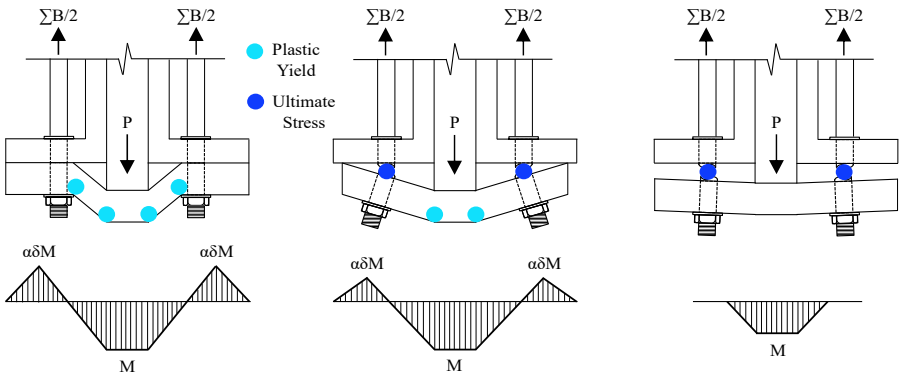

Fig. 4 Failure mode of SMA damper (Prying action)

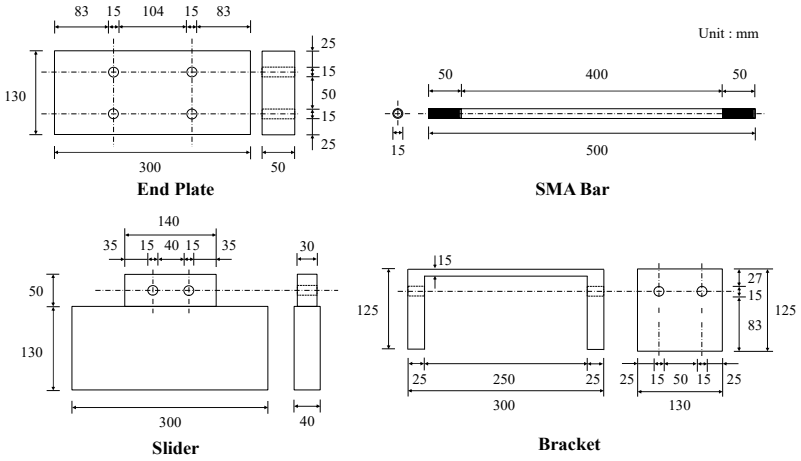

Fig. 5 Detailed sizes for all components

decreases, but the failure due to ultimate stress occurs simultaneously in SMA bars. In this case, a slight residual deformation occurs in the end plate and the SMA bars resist only part of the applied load. The occurrence of a plastic hinge on the end plate, as in failure modes 1 and 2, is called a prying action. The prying action is greatly influenced by the bending moment generated in the member supporting it by SMA bar. Therefore, it is necessary to carefully design the thickness of end plate and the distance between center line of SMA bar and slider. In general, prying action can minimized by increasing the member thickness or by reducing the distance of the location where the member resists the load.

Design details of SMA damper parts are shown in Fig. 5. Four SMA bars are manufactured with a diameter of 15 mm and a length of 500 mm. The bracket and the end plate are drilled to a depth of 50 mm and 25 mm on both sides with the same diameter as the rods, and then joined with nuts. The SMA bars are designed to avoid the heat treatment effect since the material performance is lost due to the change in material properties by welding heat. The end plate is made of 300 mm horizontal, 130 mm vertical, and 50 mm thick. The slide is made of 300 mm horizontal, 130 mm vertical, and 40 mm thick, and serves to move the end plate in the vertical direction. The joint plate is welded to the top of the slider with dimensions of 140 mm horizontal, 50 mm vertical, and 30 mm thick, and serves to transfer external loads to the slider. The bracket is installed installed between the end plates at both ends with a width of 300 mm and a height of 125 mm and prevents the SMA bars from passing through. Slider, blankets, and end plates can be made of stainless steel in areas with high corrosion but are generally made of carbon steel.

3. Response mechanism

The behaviour of the SMA specimen with pretension applied is shown in Fig. 6. As described above, the behaviour of SMA, as shown in Fig. 6(a), the ideal SMA specimen has a flag-shaped behaviour with specific recentering force (P_{Rec}). Fig. 6(b) shows the recentering behaviour due to the pretension. The initial displacement of the SMA bar by the pretension starts dissipating energy at a displacement reduced by specific recentering displacement (Δ_{Rec}). Moreover, when the pretension is applied, the strain increases. Fig. 6(c) shows the overall behaviour of SMA damper with pretension force. Fig. 7 indicates the direction of movement of the slider. The diagram is completely symmetrical because the damper is symmetrical in geometry relative to the slider to which the load of the structure is transferred. Since the initial tension force shortens the linear region, the effect of repeated loads can be reduced by increasing the initial strength. However, if the pretension is applied excessively, the energy dissipation effect is reduced because the area of the hysteresis curve becomes smaller.

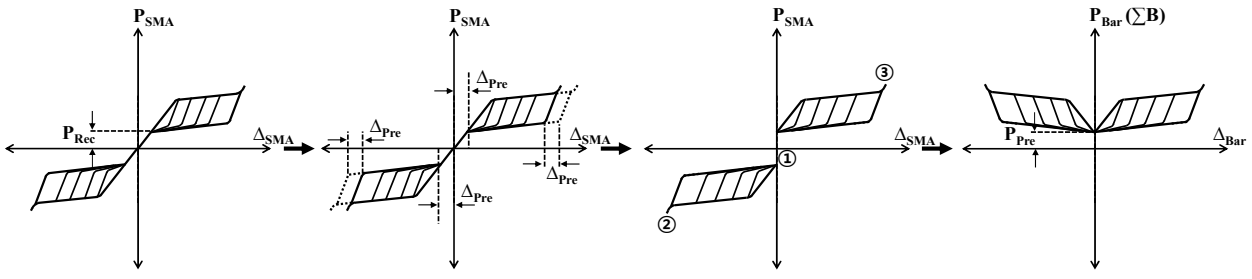

(a) Idealized SMA Behavior under Zero Pretension
(b) Idealized SMA Behavior under Initial Pretension
(c) Global Recentering Behavior of Pretensioned SMA Bars
(d) Local Reaction Behavior of Pretensioned SMA Bars

Fig. 6 Behaviour mechanism of pre-tensioned SMA bars

Therefore, the application of values exceeding half the maximum strain should be avoided. In addition, proper pretension increases the bonding strength between members, thereby avoiding the phenomenon that the SMA bar becomes loose. The reaction force of the pre-tensioned SMA bar is shown in Fig. 6(d). Since the SMA bar is always in tension, the curve appears only in the positive direction of the force axis.

Fig. 7 shows the damper movement when the load is applied. When the seismic load is transmitted through the structure to the slider of the SMA damper, the slider starts to move left and right, and the end caps move together. When the end plate moves left and right, the load is transferred to the SMA bar connected to the end cap plate, resulting in bidirectional tensile behavior. Therefore, the SMA bar of the damper is a key element that plays the role of recentering and energy dissipation by the material properties.

4. Finite element models

To understand and evaluate the damper performance, a nonlinear finite element analysis must be performed. To achieve this goal, a 3D model of the damper was simulated using commercially available ABAQUS program (Michael 2013). Fig. 8 shows the 3D FE model of the damper. The geometry of FE model was constructed from solid elements and modelled with the same dimensions as in the design. To closely observe the stress concentration of the parts, the size of each element was divided as much as possible. Since the SMA damper is completely symmetrical, half-type modelling was performed using symmetrical boundary conditions to shorten the analysis time. In addition, fixed boundary conditions were used to weld the brackets to the side plates. The material nonlinearity was considered to perform an accurate analysis in the plastic range due to cyclic loads. An elastoplastic behaviour including isotropic and kinematic strain hardening has been considered for the steel parts of the damper. The SMA material has been simulated using user material (UMAT) subroutine according to Aurrichio's model (Auricchio and Sacco 1997, Sgambitterra *et al*. 2014) and was added to the ABAQUS command prompt. This material is based on the concept of generalized plasticity and reflects superelasticity under isothermal condition (DesRoches *et al*. 2004, Lubliner and Auricchio 1996). To understand that the assembled material can work properly, an SMA specimen has been modelled in ABAQUS program and verified to DesRoches *et al*. experimental test (DesRoches *et al*. 2004). As can be seen in Fig. 9, the simulated curve has a good agreement with the experimental results.

Two load time steps were considered to individually apply the pretension and cyclic loads. The pretension is extended from the first step to the second repeated load application step. A quasi-static cyclic loading adopted from Chan and Albermani's study (Chan and Albermani 2008) has been imposed to the upper side of the slider. The pretension, a design variable, introduces load conditions that control displacements corresponding to 0, 97, 112 and 119 kN. According to the pretension, the analysis model was presented as Case-1, Case-2, Case-3, and Case-4. In

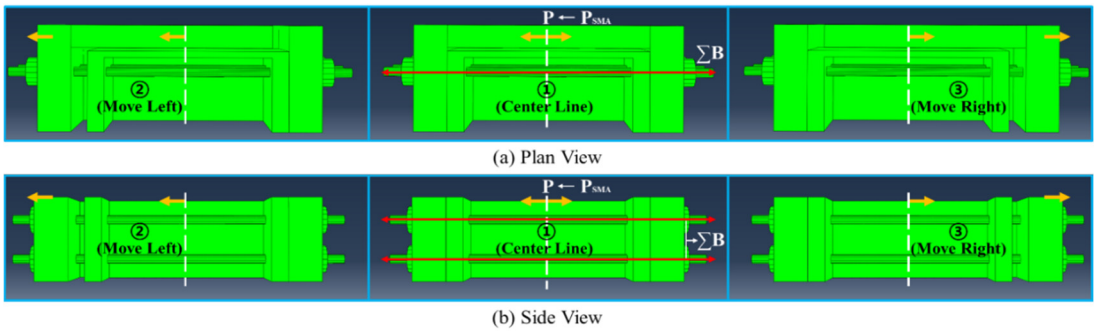

Fig. 7 Movement of SMA damper connections under cyclic loading

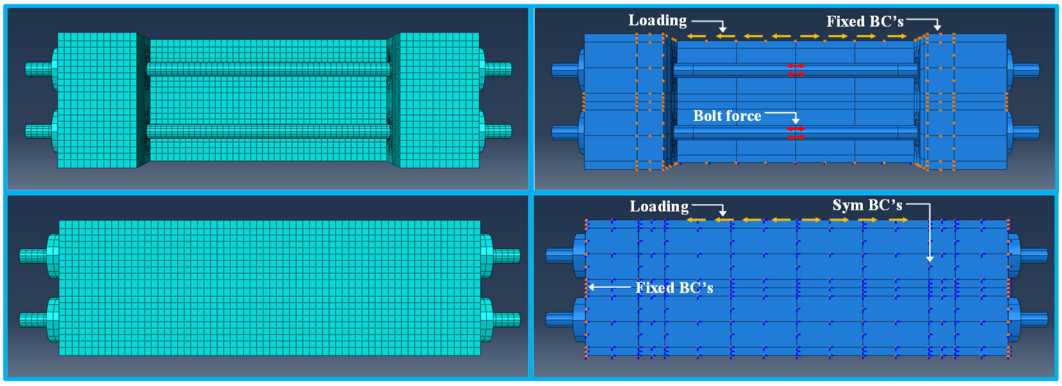

Fig. 8 Finite element models (Parts, mesh, loading, and symmetry BC's)

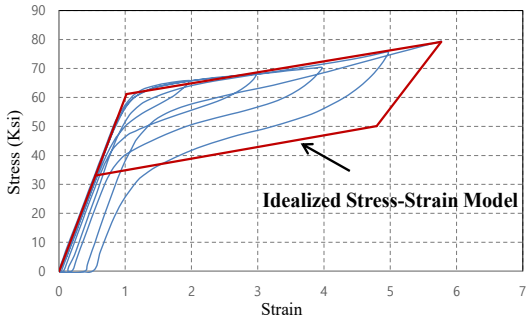

Fig. 9 Simulated stress and strain curve based on the material property of superelastic SMAs

order to prevent the rigid body from being moved by the pretension, the end plate was fixed and released before the cyclic load application step.

5. Analysis results

In this study, FEA results were analyzed to verify the performance of SMA damper with increasing pretension. Fig. 10 compares the analysis results of the SMA damper according to four design variables mentioned above.

The case-1 model without pretension applied to SMA bar is affected by material properties. Therefore, it shows a flag-shaped hysteresis curve that matches the behaviour of the SMA material. The Case-1 model was restored to an original shape after the removal of the load even if a considerable amount of deformation was applied, showing a residual displacement near zero. During the process of recentering to the original shape, a phase changing process from martensite to austenite shows a recentering Force level of about 90.5 kN.

The recentering force acts as an additional load to restore the residual displacement due to the frictional force occurring at the contact surface between the members of the damper. As the number of load cycles increases from Case-2 model to Case-4 model with increasing pretension, the residual displacement occurring tends to increase slightly. This is because the SMA bar provides recentering performance during the reverse phase displacement process to recover from a certain level of damage, but residual displacement occurs when the applied load exceeds the recentering force. However, it can be seen that the energy dissipation capacity of SMA damper increases even if the recentering is reduced. Therefore, as in the behaviour mechanism, Δ_{SMA1} to $\Delta_{SMA-max}$ a decrease in the initial tension, and the range of P_{SMA1} to $P_{SMA-max}$ shows a tendency to increase somewhat with resistance according to the increase in bonding strength. Table 1 shows the values of Δ_{SMA1} to $\Delta_{SMA-max}$ and P_{SMA1} to $P_{SMA-max}$ at specific points defined in Fig. 10. In addition, the SMA acts to reduce the residual displacement ($\Delta_{SMA-Res}$) generated in the damper to less than 3% due to the recentering performance.

Fig. 11 shows the behaviour of the bolt reaction force acting on the SMA bar affected by pretension (P_{Pre}). In case-1, the maximum force ($P_{Pre-max}$) is about 400kN, and energy dissipation begins after 2mm displacement. In Case-2, a pretension of 97 kN was applied to the SMA bar, and energy dissipation occurs simultaneously with the start. Also, the maximum force is about 80kN larger than Case-1. In case-3, degradation began, and the maximum force was about 550 kN. In case-4, more degradation occurred and energy dissipation was reduced, but the maximum performance of the damper increased to about 600 kN. In addition, by comparing the specific values of P_{SMA1}-$P_{SMA-max}$ and Δ_{SMA1}-$\Delta_{SMA-max}$ in Fig. 10 and P_{Pre1}-$P_{Pre-max}$ and Δ_{Pre1}-$\Delta_{Pre-max}$ in Fig. 11, the initial displacement of the SMA bar can be seen by the pretension as described in the behaviour mechanism.

The relationship between the bolt reaction force of the SMA bar and the applied load is shown in Fig. 12. In case-1m

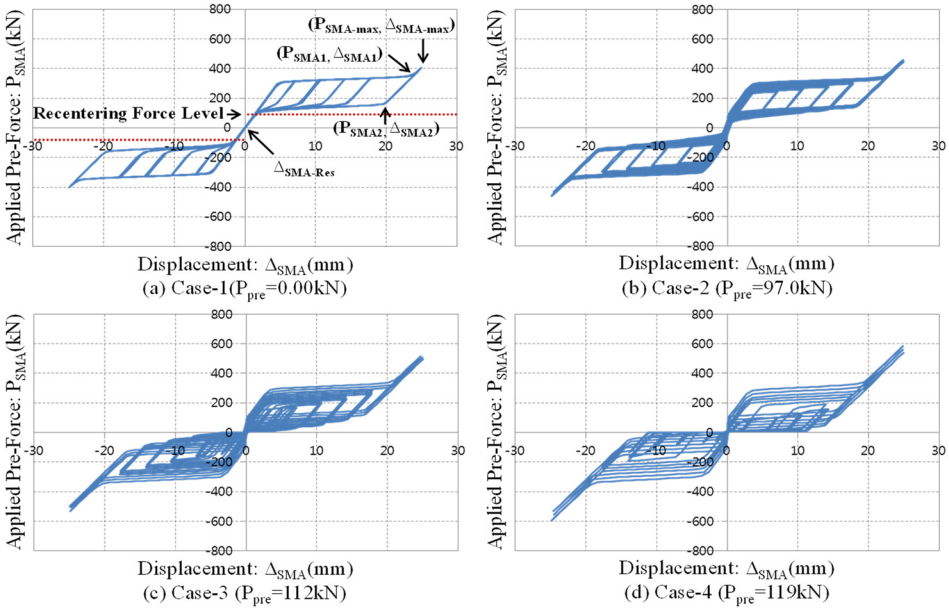

Fig. 10 FEA results for SMA damper cases

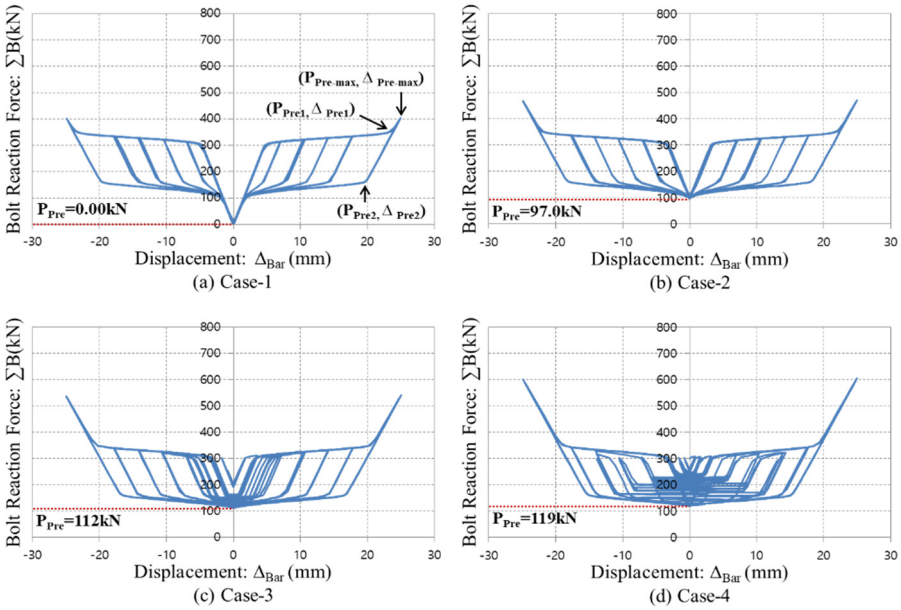

Fig. 11 Bolt reaction forces

the reaction force and load reach the ultimate load with the same value. At the beginning of the loading history, the prying action load increases by the pretension. It satisfies the equilibrium state ($P_{SMA} = \sum B$) that matches the applied load and the total bolt reaction force. In addition, the Case-1 model shows a response in which the influence of prying action, the load does not decrease as the displacement load history increases. In the case of other models, the behaviour starts in the state where the load is increased due to the increase in the pretension, and the phenomenon becomes gradually the same as the loading history increases.

In addition, as shown in Fig. 13, the curve path for each cycle was analyzed to accurately understand the relationship between bolt reaction force and displacement. The specific cycle was selected as C1 to C4 in Fig. 14(a). Cycle-1 shows that the movement by the slider is resisted by the pretension. When the damper starts to move, the holding force due to the pretension is released and the first bouncing phenomenon occurs and the bolt reaction force against the applied load increases. This is because Bolt temporarily loses the pretension. Cycle-2 and cycle-3 are getting closer to the zero-flying line, whereas the bolt reaction force and applied load are in 1:1 ratio. In cycle-4, the applied load initially increases due to the effect of pretension. It can be seen that when the end plate and bracket start to be separated by the slider, it behaves almost like a zero-frying action.

The maximum recentering displacement, which is the difference between maximum displacement and residual displacement in the last loading cycle acting on SMA

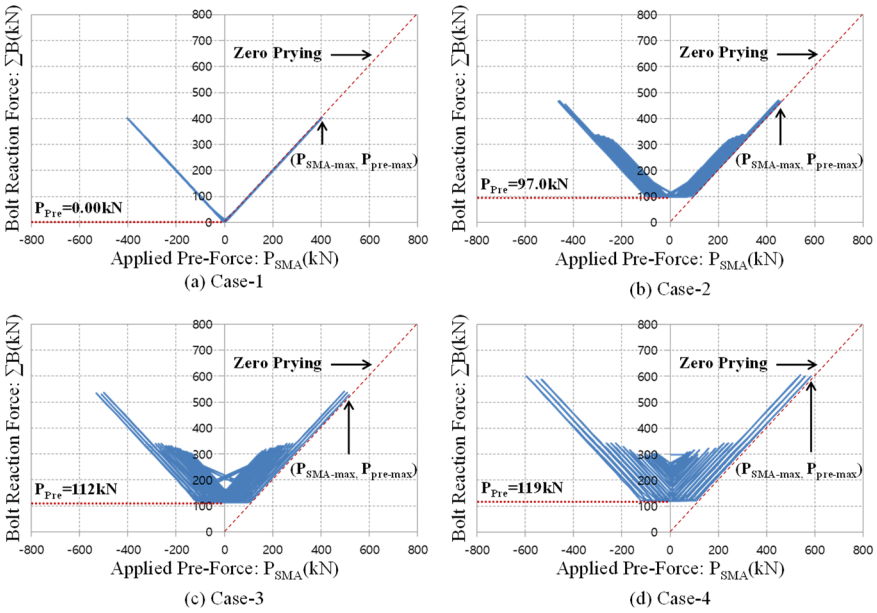

Fig. 12 Prying action (Initial force)

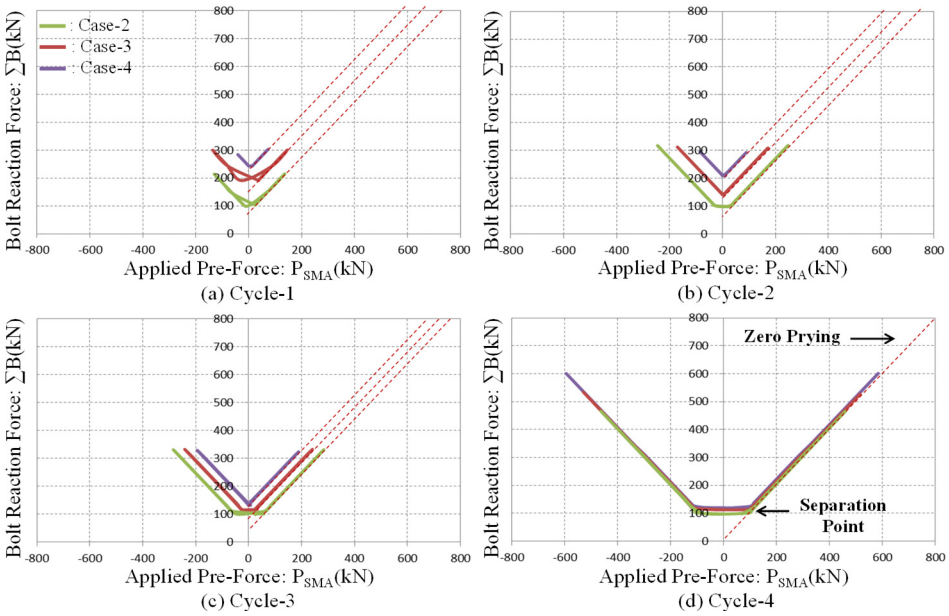

Fig. 13 Investigation of prying action in each cycle

Table 1 Analysis result of the behavior of the SMA damper

Model ID	P_{SMA1} (kN)	Δ_{SMA1} (mm)	P_{SMA2} (kN)	Δ_{SMA2} (mm)	$P_{SMA-max}$ (kN)	$\Delta_{SMA-max}$ (mm)	$\Delta_{SMA-Res}$ (mm)	RR (%)	TE (kN-mm)
Case-1	365.27	23.94	162.89	19.69	405.05	24.96	0.00	100.00	3520
Case-2	345.49	22.05	147.43	18.10	460.28	24.83	0.03	99.88	3590
Case-3	334.65	20.07	123.35	16.85	514.79	24.70	0.02	99.92	4250
Case-4	326.78	18.39	104.42	15.39	583.93	24.87	0.01	99.96	4490

damper, is required to evaluate the performance of recentering according to design parameters. Table 1 shows the specific values derived from FEA. P_{SMA1} and Δ_{SMA1} are the forces and displacements at the end of the martensite state, $P_{SMA-max}$ and $\Delta_{SMA-max}$ are the maximum displacements related to the maximum force, and P_{SMA1} and Δ_{SMA1} are the forces and displacements starting with the austenite state, respectively $\Delta_{SMA,Res}$ represents the residual displacement of each model. The recentering rate (RR), which is represented as an index for evaluating the recentering capability of the SMA damper, can be expressed as the maximum recentering displacement ($\Delta_{SMA-max} - \Delta_{SMA-Res}$) normalized to the maximum displacement ($\Delta_{SMA-max}$) as shown in Eq. (1).

$$RR = \frac{100(\Delta_{SMA-max} - \Delta_{SMA-Res})}{\Delta_{SMA-max}} \quad (1)$$

The energy dissipation capacity (TE) represents the total amount of energy generated by the overall hysteretic behaviour of the damper model and is calculated as the area of the hysteresis curve. The SMA damper has a recentering rate close to 100%. In the case-1 model, the recentering rate was 100%, and in the case-4 model, which had the highest pretension, the recentering rate was 99.96%. Since results showed an excellent recentering rate exceeding 99% for all models, it can be concluded that, the SMA bar improves the structural performance in terms of strength and recentering of the proposed damper device. It can be seen that as the pretension increases, the recentering force decreases, and the residual strain increases somewhat, but the energy dissipation capacity increases as the area of the hysteresis curve increases. This means that the SMA bar does not cause a decrease in strength in the hysteresis curve within the displacement load range. It can be seen that the energy dissipation continues to increase as the pretension increases. Due to the pretension, the SMA bar increases the load strength and dissipates a relatively large amount of energy as compared to the normal SMA. Therefore, the overall results show that the dissipated energy and the performance of damper improved when the pretension is increased.

6. Observation of field contours

It is necessary to analyze the stress and strain distribution and the stress-strain response at a specific point of the SMA damper subjected to hysteretic loop, and in order to closely observe the results of the FEA and verify its validity. Fig. 14(a) shows the hysteresis curve of displacement loading, as the number of cycles increases, the amplitude of the loaded displacement gradually increases and finally increases to a displacement of 25 mm. The displacement loading history is applied by forming a profile in the function of inputting the amplitude in the ABAQUS

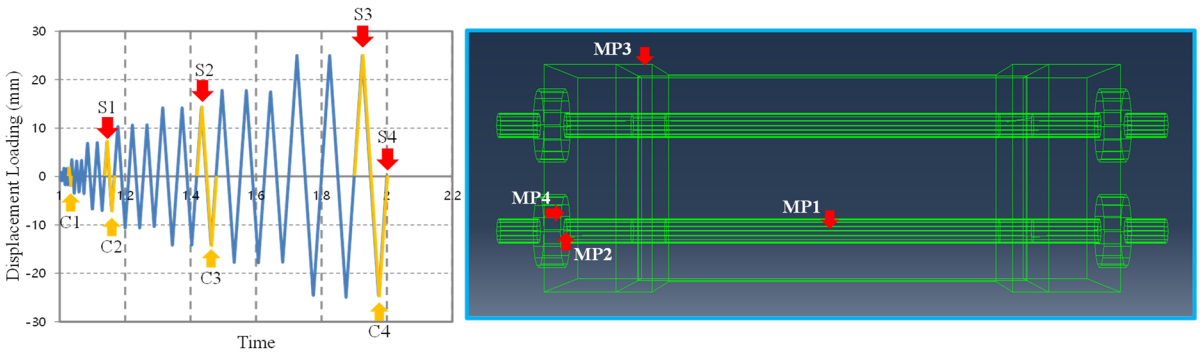

(a) Displacement Loading History (b) Measurement Points

Fig. 14 Cyclic loading history with target displacements and measurement points

program and is applied as a load in connection with boundary conditions. In addition, to examine the stress and strain distribution of the SMA damper, field contours were investigated by selecting S1 = 7, S2 = 14, S3 = 25, and S4 = 0 per cycle as specific load steps. In Fig. 14(b), the stress-strain response of the SMA damper was examined by selecting the displacement load measurement points (MP). MP1 represents a specific point in the middle of the SMA bar where tension occurs due to repeated history. MP2 represents the SMA bar connected to the nut. MP3 represents a point on the nut and MP4 represents a point on the slider.

Fig. 15 shows the typical lateral stress and strain field contours in the SMA damper for each loading step. The size of the field contour is indicated with the legend of the color bar graph. Fig. 15(a) shows the field contour of stress according to the loading step. It shows that high stress does not occur in the steel part of the damper and that most of the stress is limited to the SMA bar. Therefore, in SMA bars orange and red colors appeared, stress concentration due to tension occurs and plastic stress contour lines are distributed along the bars as the displacement load increases. In the contour, it can be seen that the largest stress close to 1,000 MPa occurs at the displacement of S = 25 mm with the largest displacement load. The SMA bar has a relatively weak stress distribution in the steel because the stress value at the stress contour is relatively high as compared to the yield strength occurring in the steel after the plastic state. In the final load step S = 0 mm, the case-1 model without pretension is restored from the previous ultimate load to a stress distribution with residual stress close to zero. In other models with initial pre-tension,

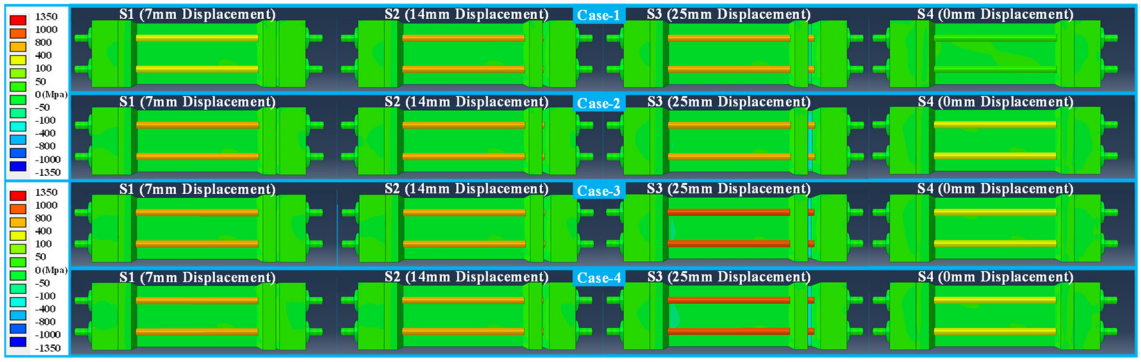

(a) Stress contour

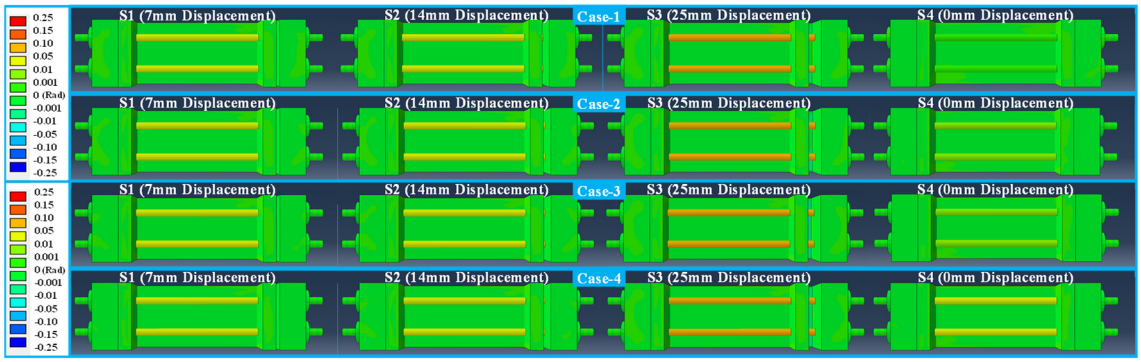

(b) Strain contour

Fig. 15 Stress and strain contour

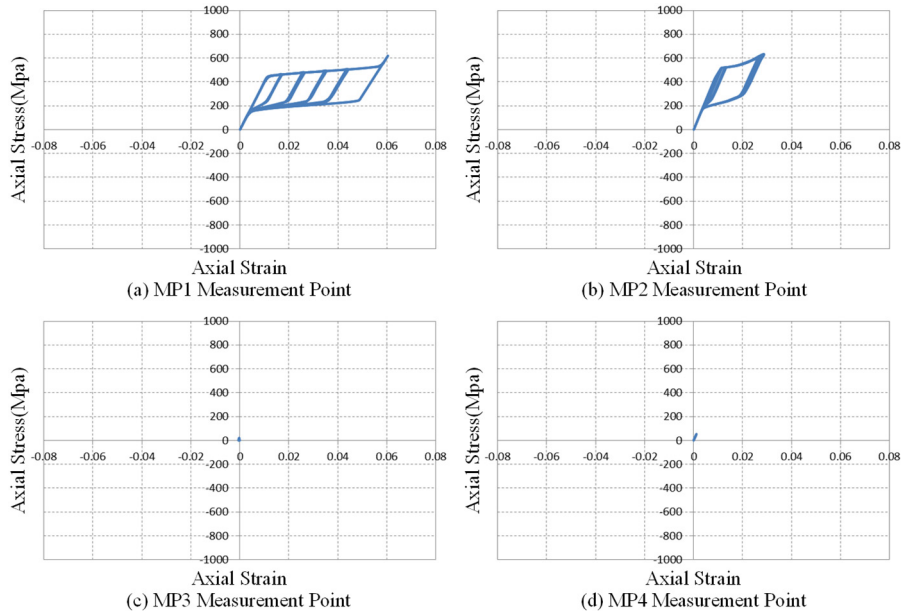

Fig. 16 Stress and strain measurement (Case-1)

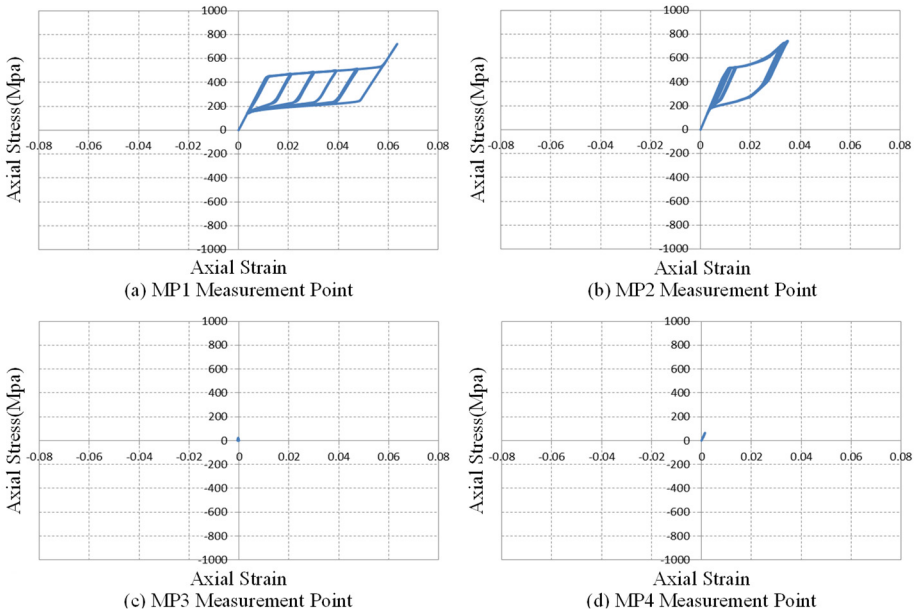

Fig. 17 Stress and strain measurement (Case-2)

residual stresses exceeding the yield level are finely distributed in yellow color on the SMA bar. This indicates that the damper can be quickly restored even after a strong earthquake.

Fig. 15(b) shows the field contour of the transverse strain according to the loading step. Similar to the stress distribution, the strain distribution due to high tension in the SMA bar, small strain distribution and plasticity pattern in yellow color appears partially due to compressive force and bending moment in other members where steel is used. In the final load step S = 0 mm, the case-1 model without pretension is restored from the load to a strain distribution with residual strain close to zero. Other models with pretensions can see the distribution of plastic patterns in orange and yellow colors in SMA bar with residual strain exceeding the yield level. Therefore, the SMA bar in the damper reduces residual stress and strain generated in the member with damper due to an increase in initial tension, and the generated size is negligible. Therefore, the SMA bar serves to stabilize the damper device and reduce residual strain.

Figs. 16-19 show the stress-strain behaviour derived from measurement points. The SMA bar acts only on the tensile load, and the stress-strain curve measured at the MP1 creates a flag-shaped hysteresis loop identical to the unique material behavior in the tensile direction only. The stress-strain curve measured at the MP2 shows similar behaviour to the curve derived at the MP1 point, but it is constrained by the nut, resulting in low strain. Numerically, the maximum stress in case-1 at the MP1 and MP2 points is

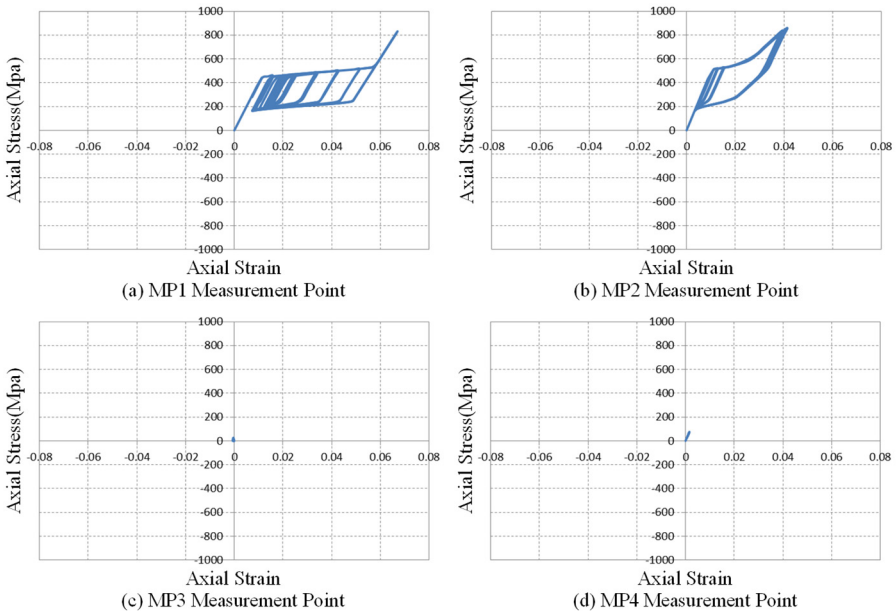

Fig. 18 Stress and strain measurement (Case-3)

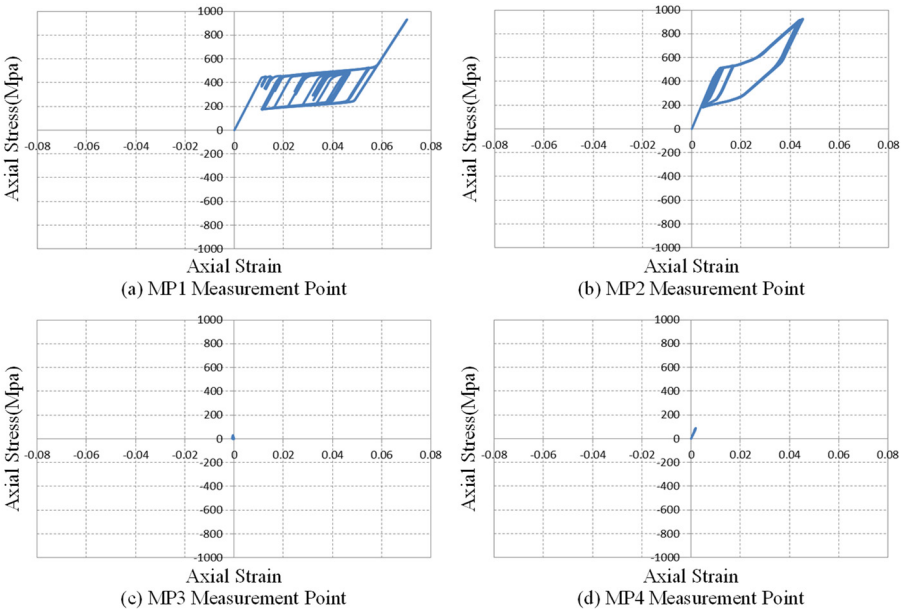

Fig. 19 Stress and strain measurement (Case-4)

about 600 kN, and the stress is stable at the MP3 and MP4 points. Also, the maximum strains are about 6 mm/mm and 3 mm/mm at the MP1 and MP2 points, while the strains at MP3 and MP4 are close to zero. In case 2, the stress and strain values increased in MP1 and MP2, and no stress and strain in MP3 and MP4. This scenario is repeated in case 3 and case 4. Therefore, as the pretension increases, the SMA bar increases the ultimate load and does not return to original shape with repeated loads and behaves under increased load. Also, it can be seen that the displacement changing from the reverse phase displacement section to the elastic range also increases. This indicates that maximum stress and strain occur in the SMA bar. The MP 3 and 4 are the points where bending moment applies remains elastic during all cyclic loads regardless of displacement. In addition, the stress values of MP1 and MP2 show that the failure of the member is limited in MP2.

7. Conclusions

In this study, to improve the recentering and energy dissipation capacity for plastic deformation, a SMA damper is proposed, that utilizes SMA capable of recentering with the material itself and applies pretension. In order to confirm the performance of the proposed damper, a behavioural response was derived by performing FEA of the damper applying the pretension to the SMA bar. In addition, the analysis results were analyzed in terms of residual strain, recentering rate, and energy dissipation capacity, and

the following conclusions were obtained.

- The design of the SMA damper determined the structural shape in order to realize the behavior principle that the load is transmitted to the shape memory alloy bar, which is the core of the damper performance. The position of the bar and the thickness of the plate, which did not cause a prying action effect, were calculated on the end plate, which is a member in contact with the SMA bar. In addition, the effectiveness of the proposed design was verified.
- The SMA damper was analyzed from the viewpoints of residual strain, recentering rate, and energy dissipation capacity according to the results of finite element analysis according to the material (shape memory alloy, steel) and pretension. As a result of analysis, the SMA damper exhibits different properties depending on the material. When the SMA is used, the residual strain is reduced even after yielding depending on the material recentering performance. However, when steel is used, due to material limitations at the beginning, a considerable amount of residual deformation occurs after plastic deformation.
- Analysis results show that the SMA damper, on average, showed a residual strain of less than 0.1 mm and a recentering rate exceeding 99%. It can be seen that residual strain occurring in the damper can be minimized by SMA's recentering effect. Furthermore, it shows excellent recentering rate and improves the structural performance in terms of damper strength and recentering force.
- The increase in the pretension, a design variable, indicates an increase in the initial modulus of elasticity and increases in yield and ultimate load, resulting in an increase in energy dissipation. After a certain amount of pretension, the recentering force decreases and stress hardening begins, but the area on the envelope of the hysteresis curve increases while some residual strain is maintained. This shows that the total energy dissipation and the maximum performance of the damper are improved.
- Therefore, the SMA damper proposed in this study should select a damper whose demanded performance is suitable according to the recentering and energy dissipation capacity. In addition, structural experiment studies will be required to verify actual performance.

Acknowledgments

This work was supported by Incheon National University Research Concentration Professors Grant in 2019.

References

Auricchio, F. and Sacco, E. (1997), "A one-dimensional model for superelastic shape-memory alloys with different elastic properties between austenite and martensite", *Int. J. Non-Linear Mech.*, **32**(6), 1101-1114. https://doi.org/10.1016/S0020-7462(96)00130-8

Chan, R.W. and Albermani, F. (2008), "Experimental study of steel slit damper for passive energy dissipation", *Eng. Struct.*, **30**(4), 1058-1066. https://doi.org/10.1016/j.engstruct.2007.07.005

DesRoches, R., McCormick, J. and Delemont, M. (2004), "Cyclic properties of superelastic shape memory alloy wires and bars", *J. Struct. Eng.*, **130**(1), 38-46. https://doi.org/10.1061/(ASCE)0733-9445 (2004)130:1(38)

Dezfuli, F.H. and Alam, M.S. (2015), "Hysteresis model of shape memory alloy wire-based laminated rubber bearing under compression and unidirectional shear loadings", *Smart Mater. Struct.*, **24**(6). https://doi.org/10.1088/ 0964-1726/24/6/065022

Gao, N., Jeon, J.S., Hodgson, D.E. and DesRoches, R. (2016), "An innovative seismic *bracing* system based on a superelastic shape memory alloy ring", *Smart Mater. Struct.*, **25**(5), 055030. https://doi.org/10.1088/0964-1726/25/5/055030

Haque, A.B.M.R. and Alam, M.S. (2017), "Hysteretic Behaviour of a Piston Based Self-centering (PBSC) Bracing System Made of Superelastic SMA Bars – A Feasibility Study", *Structures*, **12**, 102-114. https://doi.org/10.1016/j.istruc.2017.08.004

Hu, J.W. (2014), "Seismic analysis and evaluation of several recentering braced frame structures", *Proceedings of the Institution of Mechanical Engineers*, *Part C*; *J. Mech. Eng. Sci.*, **228**(5), 781-798. https://doi.org/10.1177/0954406213490600

Hu, J.W. (2015), "Response of seismically isolated steel frame buildings with sustainable lead-rubber bearing (LRB) isolator devices subjected to near-fault (NF) ground motions", *Sustainability*, **7**(1), 111-137. https://doi.org/10.3390/su7010111

Hu, J.W. and Choi, E.S. (2014), "Seismic design, nonlinear analysis, and performance evaluation of recentering buckling-restrained braced frames (BRBFs)", *Int. J. Steel Struct.*, **14**(4), 683-695. https://doi.org/10.1007 /s13296-014-1201-3

Lubliner, J. and Auricchio, F. (1996), "Generalized plasticity and shape-memory alloys", *Int. J. Solids Struct.*, **33**(7), 991-1003. https://doi.org/10.1016/0020-7683(95)00082-8

Mansouri, I., Amiri, G.G., Hu, J.W., Khoshkalam, M., Soori, S. and Shahbazi, S. (2017), "Seismic fragility estimates of LRB base isolated frames using performance-based design", *Shock Vib.*, **2017**(1), 1-20. https://doi.org/10.1155/2017/5184790

Massah, S.R. and Dorvar, H. (2014), "Design and analysis of eccentrically braced steel frames with vertical links using shape memory alloys", *Smart Mater. Struct.*, **23**(11), 115015. https://doi.org/10.1088/0964-1726/23 /11/115015

Michael, S. (2013), ABAQUS/Standard User's Manual, Version 6.13.

Mirzai, N.M. and Attarnejad, R. (2018), "Performance of EBFs equipped with an innovative shape memory alloy damper", *Scientia Iranica*. https://doi.org/10.24200/SCI.2018.50990.1955

Mirzai, N.M. and Hu, J.W. (2019), "Pilot study for investigating the inelastic response of a new axial smart damper combined with friction devices", *Steel Compos. Struct.*, *Int. J.*, **32**(3), 373-388. https://doi.org/10.12989/scs.2019.32.3.373

Mirzai, N.M., Attarnejad, R. and Hu, J.W. (2018), "Enhancing the seismic performance of EBFs with vertical shear link using a new self-centering damper", *Ing. Sismica*, **35**(4), 57-75.

Qiu, C., Gong, Z., Peng, C. and Li, H. (2020), "Seismic vibration control of an innovative self-centering damper using confined SMA core", *Smart Struct. Syst.*, *Int. J.*, **25**(2), 241-254. https://doi.org/10.12989/sss.2020.25.2.241

Sgambitterra, E., Maletta, C. and Furgiuele, F. (2014), "Modeling and simulation of the thermo-mechanical response of NiTi-based Belleville springs", *J. Intell. Mater. Syst. Struct.*, **27**(1), 81-91. https://doi.org/10.1177/1045389X14560366

Shi, F., Ozbulut, O.E. and Zhou, Y. (2019), "Influence of shape memory alloy brace design parameters on seismic performance of self-centering steel frame buildings", *J. Int. Assoc. Struct. Control Monitor.*, **27**(4). https://doi.org/10.1002/stc.2462

Silwal, B., Ozbulut, O.E. and Michael, R.J. (2016), "Seismic collapse evaluation of steel moment resisting frames with superelastic viscous damper", *J. Constr. Steel Res.*, **126**, 26-36. https://doi.org/10.1016/j.jcsr.2016.07.002

Speicher, M.S., DesRoches, R. and Leon, R.T. (2017), "Investigation of an articulated quadrilateral bracing system utilizing shape memory alloys", *J. Constr. Steel Res.*, **130**, 65-78. https://doi.org/10.1016/j.jcsr.2016.11.022

Sultana, P. and Youssef, M.A. (2016), "Seismic performance of steel moment resisting frames utilizing superelastic shape memory alloys", *J. Constr. Steel Res.*, **125**, 239-251. https://doi.org/10.1016/j.jcsr.2016.06.019

Sultana, P. and Youssef, M.A. (2018), "Seismic performance of modular steel frames equipped with shape memory alloy braces", *Bull. Earthq. Eng.*, **16**(11), 5503-5527. https://doi.org/10.1007/s10518-018-0394-9

Zareie, S., Mirzai, N., Alam, M.S. and Seethlaer, R.J. (2017), "A dynamic analysis of a novel shape memory alloy based bracing system", *CSCE-SCGC 2017 Annual General Conference*, Vancouver, BC, Canada, May.

Zareie, S., Alam, M.S., Seethaler, R.J. and Zabihollah, A. (2019), "A shape memory alloy-magnetorheological fluid core bracing system for civil engineering applications: a feasibility study", *Proceedings of the 7th International Specialty Conference on Engineering Mechanics and Materials*, Montreal, Canada, June.

HJ